

Metadata of the chapter that will be visualized online

Book Title	Encyclopedia of Computer Vision	
Book Copyright Year	2013	
Copyright Holder	Springer Science+Business Media, LLC	
Title	Shock Graph	
Author	Degree	Prof.
	Given Name	Sven J.
	Particle	
	Family Name	Dickinson
	Suffix	
	Phone	
	Fax	
	Email	sven@cs.toronto.edu
Affiliation	Division	Department of Computer Science
	Organization	University of Toronto
	Street	6 King's College Rd.
	City	Toronto
	State	ON
	Country	Canada
Author	Degree	Dr.
	Given Name	Ali
	Particle	
	Family Name	Shokoufandeh
	Suffix	
	Phone	
	Fax	
	Email	ashokouf@cs.drexel.edu
Affiliation	Division	Department of Computer Science
	Organization	Drexel University
	Street	3141 Chestnut St.
	Postcode	19104
	City	Philadelphia
	State	PA
	Country	USA

Author	Degree	Dr.
	Given Name	Kaleem
	Particle	
	Family Name	Siddiqi
	Suffix	
	Phone	
	Fax	
	Email	siddiqi@cim.mcgill.ca
Affiliation	Division	School of Computer Science
	Organization	McGill University
	Street	3480 University Street
	Postcode	H3A 2A7
	City	Montreal
	State	PQ
	Country	Canada

Corrected Proof

S

Shock Graph

- 1 Sven J. Dickinson¹, Ali Shokoufandeh² and Kaleem
 2 Siddiqi³
 3 ¹Department of Computer Science, University of
 4 Toronto, Toronto, ON, Canada
 5 ²Department of Computer Science, Drexel University,
 6 Philadelphia, PA, USA
 7 ³School of Computer Science, McGill University,
 8 Montreal, PQ, Canada

9 Related Concepts

- 10 ▶ [Grassfire Flow](#); ▶ [Graph Matching](#); ▶ [Medial](#)
 11 [Axis/Skeleton](#); ▶ [Many-to-Many Graph Matching](#);
 12 ▶ [Object Categorization](#)

13 Definition

14 The shock graph is obtained from the 2D Blum medial
 15 axis by incorporating properties of the radius func-
 16 tion along the skeleton. The direction in which the
 17 radius function increases, or equivalently, the direc-
 18 tion of the grassfire flow, is used to order groups of
 19 skeletal points and to derive parent-child relationships.
 20 This results in a directed acyclic graph whose nodes
 21 represent skeletal points and whose edges represent
 22 adjacency relationships. A variant of this construction
 23 associates skeletal points with edges, with the nodes
 24 representing the adjacencies.

Background

25

When Blum conceived of the medial axis or skele- 26
 ton, his goal was to use it as a means to categorize 27
 objects from their projected (2D) outlines [4]. Specifi- 28
 cally, by associating the direction of increasing radius 29
 value along a skeletal branch, or equivalently the direc- 30
 tion of propagation of singularities of the grassfire flow, 31
 he proposed the concept of an axis-morphology or *a-* 32
morph by which to achieve object categorization. His 33
 basic insight was that this could lead to a decomposi- 34
 tion that reflected the qualitative part structure of the 35
 object. As an example, ignoring their detailed bound- 36
 ary geometry, outlines of hands would have similar 37
a-morphs and these would be quite distinct from those 38
 of outlines of humans, fish or other object classes. In 39
 fact, he drew upon these later examples towards the 40
 end of his classic paper [4], where he also sketched 41
 possible extensions to 3D. 42

Whereas much has been written about medial or 43
 skeletal representations over the years (see [23] and 44
 also the medial axis/skeleton entry in this encyclope- 45
 dia) the idea that an *a-morph* was essentially a directed 46
 graph which could be used for object recognition 47
 caught on only in the early 1990s. One likely reason 48
 is that it took the image analysis and computer vision 49
 communities many years to develop robust algorithms 50
 for skeleton computation. Since this time, however, a 51
 variety of successful approaches to view-based recog- 52
 nition using shock-graphs have been proposed and 53
 have been validated on large databases. Several of 54
 these are described in the present entry. There also 55
 exist more recent variants of the shock graph, such 56
 as Macrini et al.'s bone graph [14], which attempt to 57

58 mitigate the representational instability of the Blum
59 medial axis. In fact, the mapping of the Blum skele-
60 ton to a graph-based representation, of which the shock
61 graph is the most widely researched example, remains
62 an active area of investigation.

63 Theory

64 The Blum medial axis or skeleton of a 2D outline
65 is homotopic to it and is comprised of three types
66 of skeletal points: endpoints of skeletal curves, inte-
67 rior points and branch points. The branch points are
68 generically of degree 3, i.e., three skeletal curves are
69 connected at a branch point. A formal classification
70 is presented in [11]. The shock graph takes the 2D
71 skeleton of a simple closed curve as input (one with-
72 out holes) and labels each skeletal point according to
73 whether the radius function at it is increasing mono-
74 tonically (a 1-shock), is a local minimum (a 2-shock),
75 is constant (a 3-shock) or is a local maximum (a
76 4-shock). Groups of adjacent 1-shocks are considered
77 together, as are groups of 3-shocks. Given this interpre-
78 tation, a directed acyclic graph is obtained by consider-
79 ing the skeletal points with the largest radii, which are
80 the last to form in the grassfire flow, as the children of a
81 dummy root node. The children are then placed, recur-
82 sively, in order of decreasing radius value. This process
83 of reversing the grassfire flow and adding 1-shock
84 groups or 3-shock groups as children, is governed by
85 the rules of a grammar, as shown in [24].

86 Rather than provide all the details of the grammar
87 in this entry, the reader is referred to the examples
88 in Fig. 1, which show the construction of the shock
89 graphs of two brush shapes. The medial axis of each
90 object is shown in the bottom row, with distinct groups
91 of shocks being given a unique color (3-shocks are
92 shown in yellow). In the labeling, the shock type
93 appears first, followed by a unique identifier. The asso-
94 ciated shock graphs are shown in the top row. It is
95 clear that each shape is abstracted by a single root
96 node (the 3-shock group describing the elongated por-
97 tion of the brush), with its children being additional
98 protrusions (1-shock groups). One of these protrusions
99 has a 3-shock group as a child, which describes the
100 handle of each brush. From this example it is evident
101 that the shock graph is a formalization of Blum's a-
102 morph, with the advantage that it lends itself to the use

of graph-based methods for object categorization, as 103
detailed below. 104

It is also important to point out that there is a variant 105
of the shock graph where the representation places the 106
skeletal points at edges of the graph, with the nodes 107
representing connections. This variant is described in 108
detail in [18, 19]. This representation has lead to dif- 109
ferent but equally successful methods for object recog- 110
nition, based on a notion of the edit-distance between 111
two graphs. The results of using this approach are also 112
briefly described below. 113

Shock Graph-Based Object Categorization 114

An object categorization system based on shock graphs 115
consists of two components: (1) an indexing compo- 116
nent, which takes an input shock graph and returns, 117
from a large database of model shock graphs, a small 118
number of candidate shock graphs that might account 119
for the input; and (2) a matching component, which 120
takes one of the candidates and the input, and com- 121
putes a similarity (or distance), along with a set of node 122
correspondences. Under ideal conditions, the input 123
shock graph would contain no artifacts due to noise, 124
occlusion, or clutter, and would be isomorphic to one 125
of the model shock graphs (provided that the input 126
object represents one of the model objects). However, 127
such conditions are highly unlikely, for in addition to 128
noise, occlusion, and scene clutter, ligature-induced 129
instabilities [1] often lead to spurious nodes/edges as 130
well as medial branch oversegmentation. Formulating 131
the problem as graph isomorphism, subgraph isomor- 132
phism, or even largest isomorphic subgraph will not 133
lead to a meaningful solution, for large, or even signif- 134
icant isomorphisms may simply not exist between two 135
shock graphs that represent instances of the same cat- 136
egory. The shock graph indexing and matching prob- 137
lems are therefore inexact graph indexing/matching 138
problems. 139

Indexing Shock Graphs 140

Given an input shock graph, the goal of the index- 141
ing module is to quickly (sublinearly) retrieve a small 142
number of candidate model database shock graphs 143
among which the input is likely included. As men- 144
tioned above, the input shock graph may be corrupted 145
in a number of ways, precluding a simple global (based 146

147 on the entire input) indexing framework. For example:
 148 (1) occlusion may remove part of the input shock graph
 149 and replace the missing part with a shock graph (or
 150 subgraph) belonging to a different object; (2) shadows
 151 or poor illumination may simply delete some portion of
 152 the input shock graph; (3) scene clutter may embed the
 153 object shock graph (or portion thereof) in a much larger
 154 “scene” shock graph; and (4) ligature-based instabil-
 155 ity may introduce spurious nodes or may overpartition
 156 other nodes in the input shock graph. These factors
 157 require a part-based indexing framework that can oper-
 158 ate in the presence of noise, occlusion, clutter, and
 159 ligature-based instability.

160 One such indexing framework that is applicable
 161 to not only shock graphs but any hierarchical, graph-
 162 based representation (specifically, any directed acyclic
 163 graph-based representation) was introduced by Shoko-
 164 ufandeh et al. [22], originally for the purpose of shock
 165 graph indexing. The key concept behind the approach
 166 is to capture the abstract shape of a graph (or subgraph)
 167 with a low-dimensional vector, yielding an efficient
 168 indexing mechanism. Capturing the abstract shape of a
 169 graph is important so that the index is invariant to noise
 170 and minor within-class shape deformation. Indexing at
 171 the part level is important in the presence of occlusion
 172 and scene clutter. Mapping a discrete graph structure
 173 to a low-dimensional point facilitates a simple nearest-
 174 neighbor search in a geometric space for similar model
 175 parts which, in turn, can vote for those model objects
 176 that contain those parts. Those model objects receiv-
 177 ing the largest votes represent those candidate objects
 178 passed to the shock graph matching module for a more
 179 detailed analysis.

180 The graph-based shape abstraction is computed
 181 at every non-leaf node, and captures the abstract
 182 “shape” of the underlying subgraph rooted at that
 183 node. Therefore, each non-leaf node (with only four
 184 shock graph node types, leaf nodes are far too
 185 uninformative/ambiguous) “votes” for those objects
 186 that share its substructure; the root of the graph would
 187 therefore vote at the object level, and would be mean-
 188 ingful only if the object were unoccluded and not
 189 embedded in a larger scene. Mapping the structure of a
 190 rooted subgraph to a vector assigned to the subgraph’s
 191 root is based on a spectral analysis of the graph’s struc-
 192 ture. The eigenvalues of a graph’s adjacency matrix
 193 (whose values are 0,1,-1) capture important proper-
 194 ties of the degree distribution of the graph’s nodes.

195 The eigenvalues can be combined to yield a low-
 196 dimensional abstraction of the graph’s shape in terms
 197 of how and where the edges are distributed throughout
 198 the graph. Moreover, such a spectral “signature,” called
 199 the *topological signature vector*, is proven to be sta-
 200 ble under minor perturbations of graph structure due to
 201 noise. Details of the approach are found in [22], while
 202 an application of the same indexing framework to a
 203 different hierarchical graph, specifically a 3-D medial
 204 surface graph, can be found in [25].

Matching Shock Graphs

205 Given two shock graphs, e.g., one representing the
 206 input and one representing a model candidate, the
 207 matching component needs to return not only a similar-
 208 ity or distance measure that can be used to rank order
 209 the candidates, but also an explicit correspondence that
 210 defines which model nodes correspond to which input
 211 nodes. Such correspondence is necessary, for in the
 212 case of a cluttered scene, those nodes found to match a
 213 given model would be removed, and another candidate
 214 model matched to the remaining nodes. Moreover, the
 215 correspondence need not be one-to-one, for in the case
 216 of ligature-induced medial branch oversegmentation,
 217 node correspondence may be *many-to-many*.
 218

219 Siddiqi et al. [24] developed a matching algorithm
 220 for shock graphs which, like the indexing framework
 221 of Shokoufandeh et al. [22] discussed above, can be
 222 applied to the matching of any directed acyclic graph
 223 structure, provided that a domain-dependent node sim-
 224 ilarity function is given. The algorithm is based on the
 225 same spectral graph theoretic abstraction that forms
 226 the heart of the indexing component described above.
 227 The algorithm formulates the matching of two graphs
 228 as finding a maximal matching in a bipartite graph
 229 over the two nodes sets (input and model). The edge
 230 weights (each spanning one input shock graph node
 231 and one model shock graph node) in the graph have
 232 two components: (1) the distance between the two
 233 nodes’ respective topological similarity vectors, defin-
 234 ing the similarity of their underlying graph structures
 235 (rooted at the two nodes); and (2) a node similar-
 236 ity function (the only domain-dependent component
 237 of the algorithm) that defines the similarity of the
 238 node attributes (for shock graphs, this encodes the geo-
 239 metric similarity between the two skeletal branches
 240 corresponding to the two nodes).

241 At first glance, the matching algorithm would seem
 242 to throw out all the important hierarchical structure in
 243 the two graphs (absent in the bipartite graph); nodes in
 244 one graph are matched to nodes in the other graph, but
 245 the edges in the two original graphs appear to play no
 246 role. However, the key contribution of the algorithm is
 247 that the hierarchical edge structure is brought back via
 248 the topological signature vector similarity term. For the
 249 bipartite matching algorithm to match two nodes (i.e.,
 250 select that edge in the matching), both their geomet-
 251 ric similarity and their topological similarity must be
 252 high. In other words, the contents of the two nodes
 253 must be similar and the subgraphs rooted at the two
 254 nodes must be similar. The algorithm iterates by com-
 255 puting a matching, selecting the best edge from the
 256 matching (having maximum similarity), adding it to
 257 the solution set, and recursively continuing the pro-
 258 cess on the remaining graphs (after removing the pair
 259 of matching nodes defined by the best edge). Details
 260 of the approach are found in [24], while its applica-
 261 tion to other shape matching problems is described in
 262 [21] (multiscale blob and ridge graphs), [25] (medial
 263 surface graphs), and [8, 26] (curve skeleton graphs).

264 The above algorithm eventually yields a one-to-
 265 one node correspondence between the two graphs.
 266 However, because the algorithm generates the node
 267 correspondence in a coarse-to-fine manner, stopping
 268 the algorithm at the level of a coarse node-to-node cor-
 269 respondence defines an explicit many-to-many corre-
 270 spondence between the nodes in the subgraphs rooted
 271 at the coarse nodes. Moreover, since the topological
 272 signature vectors are stable under small amounts of
 273 additive graph noise, similarity can remain high even
 274 though the two subgraphs may have different numbers
 275 of nodes. As the cardinalities of the two graphs' node
 276 sets begin to differ more dramatically, for example
 277 due to heavy under- or over-segmentation, the method
 278 breaks down and more powerful many-to-many graph
 279 matching must be employed.

280 One such method for many-to-many graph match-
 281 ing of medial axis-based graphs was proposed by
 282 Demirci et al. [9, 10]. Their algorithm transforms the
 283 graphs into a finite dimension metric space in which
 284 an approximate solution to the many-to-many match-
 285 ing problem becomes tractable. The embedding step
 286 will result in a set of points, each representing a vertex
 287 of the original graph. Their proposed embedding has
 288 the additional property that pairwise distances between
 289 points in the target metric space closely resemble

the shortest-path distances between the corresponding 290
 nodes in the graphs. Matching two graphs can then 291
 be formulated as the problem of matching their two 292
 embeddings. The many-to-many matching of the two 293
 embeddings then can be computed by solving a trans- 294
 portation problem using the Earth Mover's Distance 295
 algorithm [7]. The solution of this latter problem com- 296
 puts the mass which flows from one weighted point 297
 set to another that minimize the total transportation 298
 cost. The computed flows, in turn, define the many- 299
 to-many node correspondences between the original 300
 graphs. 301

The problem of matching shock graphs has also 302
 been studied in the context of edit-distance meth- 303
 ods [18, 29]. These algorithms estimate the cost of 304
 matching as a function of edit operations, including 305
 node relabelings, additions and deletions, and edge 306
 contraction that transform one graph into another. 307
 A fundamental issue in devising algorithms based on 308
 edit-distance is the choice of cost of each operation. 309
 Torsello and Hancock [29] use the heuristic proposed 310
 by Bunke [5] for the cost associated with their edit 311
 operations. For example, the cost of relabeling ele- 312
 ments is less than the cost of performing a deletion 313
 followed by inserting a new node with a new label. 314
 In contrast, Sebastian et al. [18] propose a multi- 315
 step heuristic to derive their edit costs. Their overall 316
 heuristic is centered around the notion of a shape cell, 317
 i.e., a collection of shapes which have identical shock 318
 graph topology. They define the cost of the deforma- 319
 tion operation as a function of the discrepancy between 320
 matching shock attributes of shapes within a given 321
 cell. The cost associated with other edit operations is 322
 derived as the limit of the deformation cost when a 323
 shape moves to the boundary a shape cell. 324

Caelli and Kosinov [6] show how inexact matching 325
 can be utilized for measuring shape similarity between 326
 shock graphs. Their method establishes correspon- 327
 dence between sets (clusters) of vertices of two given 328
 graphs and as such can be viewed as a many-to-many 329
 matching approach. Their algorithm can be viewed as 330
 a generalization of the approach of Scott and Longuet- 331
 Higgins [17]. The actual matching is established using 332
 the renormalization of projections of vertices into the 333
 eigenspaces of graphs combined with a form of rela- 334
 tional clustering. Similar to other inexact matching 335
 algorithms, their eigenspace renormalization projec- 336
 tion clustering method is able to match graphs with 337
 different numbers of vertices. 338

339 Experimental Results

340 This section presents some examples of shock graphs
 341 and their matchings using the approaches described
 342 above. [Figure 1](#)(top) illustrates two shock graphs,
 343 describing different views of a brush, computed by
 344 the algorithm of Siddiqi et al. [24]. The underlying
 345 shocks, along with the computed matchings between
 346 segments (nodes), are shown in [Fig. 1](#)(bottom). [Fig-](#)
 347 [ure 2](#) represents the ability of the algorithm to compare
 348 objects based on their prototypical or coarse shape.
 349 Here, columns 2 through 10 denote the prototype views
 350 for each of nine object classes. The similarity between
 351 the prototypes and some of the objects in the database
 352 is reflected in the rows of this table. For each row, a
 353 box has been placed around the most similar shape.
 354 Demirci et al. [9] also evaluated the effectiveness of
 355 their matching algorithm for shape retrieval based on
 356 shock graphs from the Rutgers Tool Database [24].
 357 [Figure 3](#) shows some examples of the many-to-many
 358 feature matching results obtained from the algorithm
 359 for some of the objects in the Rutgers Tools Database.
 360 Finally, [Fig. 4](#) shows the results obtained from apply-
 361 ing the edit-distance algorithm of Sebastian et al. [18]
 362 to the matching of shock segments. Note that their
 363 edit distance algorithm will also produce a sequence
 364 of intermediate shock graphs that identify the steps of
 365 the transformation of one input shock graph to another.

366 Challenges

367 Symmetry is a powerful shape regularity that has
 368 formed the basis of many shape representations,
 369 including generalized cylinders [3], superquadrics
 370 [16], and geons [2]. Just as geons provide a quali-
 371 tative and discrete shape abstraction of a generalized
 372 cylinder, shock graphs provide a discrete and qualita-
 373 tive shape abstraction of a medial axis. The resulting
 374 graph is ideally suited to shape categorization, for it
 375 is part-based, is stable under within-class deforma-
 376 tion, and is stable under part articulation. However,
 377 the shock graph also faces some important challenges.
 378 First of all, it assumes that a closed contour has been
 379 recovered from an image, separating figure from back-
 380 ground. While figure-ground segmentation remains an
 381 open research problem, it is important to note that in

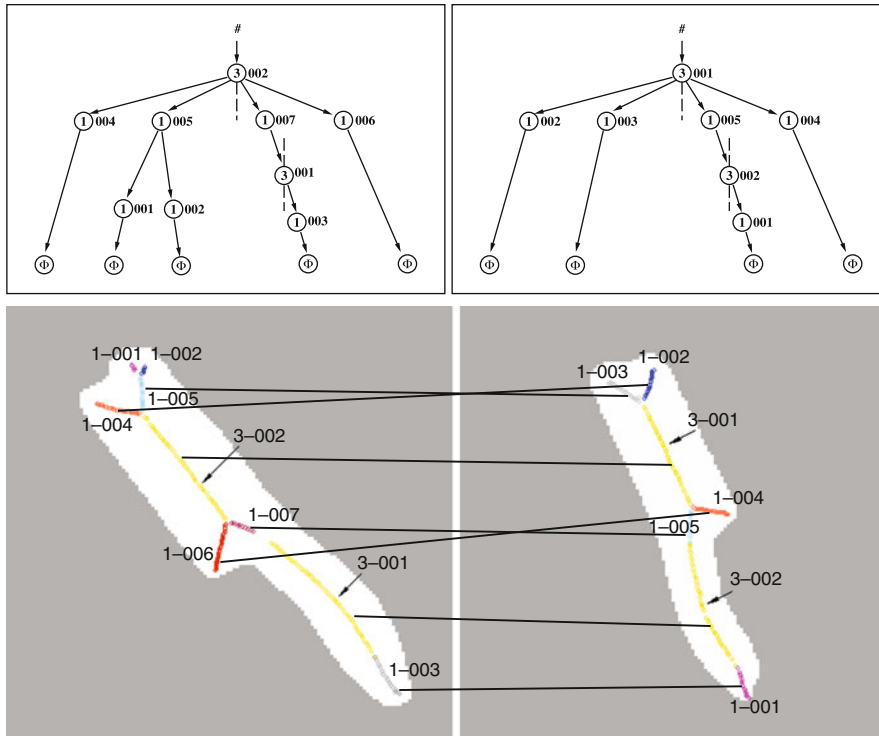
a categorization system, a perfect figure-ground sep- 382
 aration may not be necessary. If a significant portion 383
 of the figure’s boundary is correctly segmented, a 384
 significant portion of the resulting shock graph may 385
 be correct – enough to yield the correct candidate 386
 (among the list of returned candidates) during index- 387
 ing. Still, while a shock graph does preserve locality of 388
 representation, significant figure-ground segmentation 389
 errors can propagate through the representation, dis- 390
 rupting it to a degree that prevents effective indexing. 391
 A recent attempt to recover a symmetric part decom- 392
 position from a cluttered scene has been reported by 393
 Levinshtein et al. [13], in which symmetric parts are 394
 detected locally (bottom-up) and then grouped to form 395
 an approximation to a medial axis. 396

The second challenge facing the shock graph is the 397
 ligature-based instability discussed earlier [1]. A num- 398
 ber of approaches exist to try and regularize the medial 399
 axis through boundary smoothing, e.g., [12, 20, 27]; 400
 however, these methods do not effectively address 401
 the ligature structure. Other methods have sought to 402
 abstract the medial axis by regularizing out small 403
 internal branches, e.g., [28, 30]; however these meth- 404
 ods don’t explicitly target ligature structure. A recent 405
 promising approach to abstracting out ligature struc- 406
 ture is proposed by Macrini et al. [14, 15], yielding 407
 a representation, called the *bone graph*, whose parts 408
 are the non-ligature medial branches that represent the 409
 salient parts and whose edges represent the “glue” 410
 (defined by the ligature branches) that binds the parts. 411

References




















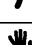




1. August J, Siddiqi K, Zucker S (1999) Ligature instabili- 413
ties in the perceptual organization of shape. *CVIU* 76(3): 414
231–243 415
2. Biederman I (1985) Human image understanding: Recent 416
research and a theory. *Comput Vis Graph Image Process* 417
32:29–73 418
3. Binford TO (1971) Visual perception by computer. In: Pro- 419
ceedings of the IEEE conference on systems and control, 420
Miami 421
4. Harry Blum (1973) Biological shape and visual science. *J* 422
Theor Biol 38:205–287 423
5. Bunke H (1997) On a relation between graph edit distance 424
and maximum common subgraph. *Pattern Recognit Lett* 425
18(8):689–694 426
6. Caelli T, Kosinov S (2004) An eigenspace projection clus- 427
tering method for inexact graph matching. *IEEE Trans* 428
Pattern Anal Mach Intell 26(4):515–519 429

- 430 7. Cohen SD, Guibas LJ (1999) The earth mover's distance
431 under transformation sets. In: Proceedings of the interna-
432 tional conference on computer vision (ICCV), Kerkyra, pp
433 1076–1083
- 434 8. Cornea N, Demirci MF, Silver D, Shokoufandeh A, Dick-
435 inson S, Kantor P (2005) 3d object retrieval using many-
436 to-many matching of curve skeletons. In: Proceedings of
437 the international conference on shape modeling and appli-
438 cations (SMI), MIT, Cambridge, pp 368–373
- 439 9. Denirci MF, Shokoufandeh A, Keselman Y, Bretzner L,
440 Dickinson S (2006) Object recognition as many-to-many
441 feature matching. *Int J Comput Vis* 69(2):203–222
- 442 10. Demirci F, Shokoufandeh A, Dickinson S (2009) Skeletal
443 shape abstraction from examples. *IEEE Transactions on Pat-
444 tern Analysis and Machine Intelligence (PAMI)*, 31(5):944–
445 952
- 446 11. Giblin Peter J, Kimia Peter J (2003) On the local form and
447 transitions of symmetry sets, medial axes, and shocks. *IJCV*
448 54(1–3):143–157
- 449 12. Katz Robert A, Pizer Stephen M (2003) Untangling the
450 blum medial axis transform. *Int J Comput Vis* 55(2–3):
451 139–153 .
- 452 13. Levinshtein A, Sminchisescu C, Dickinson S (2009) Multi-
453 scale symmetric part detection and grouping. In: Proceed-
454 ings of the international conference on computer vision
455 (ICCV), Kyoto
- 456 14. Macrini D, Dickinson S, Fleet D, Siddiqi K (2011) Bone
457 graphs: Medial shape parsing and abstraction. *Comput Vis
458 Image Underst (CVIU)*, special issue on graph-based repre-
459 sentations, Special Issue on Graph-Based Representations,
460 115(7):1044–1061
- 461 15. Macrini D, Dickinson S, Fleet D, Siddiqi K (2011) Object
462 categorization using bone graphs. *Computer Vision and
463 Image Understanding (CVIU)* 115(8):1187–1206
- 464 16. Pentland A (1986) Perceptual organization and the represen-
465 tation of natural form. *Artif Intell* 28:293–331
- 466 17. Scott G, Longuet-Higgins H (1991) An algorithm for asso-
467 ciating the features of two patterns. *Proceedings of royal
468 society of london B*244:21–26
- 469 18. Sebastian T, Klein P, Kimia B (2001) Recognition of shapes
470 by editing shock graphs. In: Proceedings of the interna-
471 tional conference on computer vision (ICCV), Vancouver
472 755–762
19. Sebastian T, Klein P, Kimia B (2004) Recognition of shapes 473
by editing shock graphs. *IEEE Trans Pattern Anal Mach* 474
Intell 26:550–571 475
20. Doron Shaked, Bruckstein Alfred M (1998) Pruning medial 476
axes. *Comput Vis Image Underst* 69(2):156–169 477
21. Shokoufandeh A, Bretzner L, Macrini D, Demirci MF, 478
Jönsson C, Dickinson S (2006) The representation and 479
matching of categorical shape. *Comput Vis Image Underst* 480
103(2):139–154 481
22. Shokoufandeh A, Macrini D, Dickinson S, Siddiqi K, 482
Zucker SW (2005) Indexing hierarchical structures using 483
graph spectra. *IEEE Trans Pattern Anal Mach Intell* 484
27(7):1125–1140 485
23. Siddiqi K, Pizer Stephen M (2008) Medial representa- 486
tions: mathematics, algorithms and applications. Springer, 487
Dordrecht 488
24. Siddiqi K, Shokoufandeh A, Dickinson S, Zucker S (1999) 489
Shock graphs and shape matching. *Int J Comput Vis* 30:
490 1–24 491
25. Siddiqi K, Zhang J, Macrini D, Shokoufandeh A, Bioux S, 492
Dickinson S (2008) Retrieving articulated 3-d models using 493
medial surfaces. *Mach Vis Appl* 19(4):261–275 494
26. Sundar H, Silver D, Gagvani N, Dickinson S (2003) Skele- 495
ton based shape matching and retrieval. In: Proceedings 496
of the international conference on shape modelling and 497
applications (SMI), Seoul, pp 130–142 498
27. Hüseyin Tek, Kimia Benjamin B (2001) Boundary smooth- 499
ing via symmetry transforms. *J Math Imaging Vis* 500
14(3):211–223 501
28. Telea A, Sminchisescu C, Dickinson S (2004) Optimal 502
inference for hierarchical skeleton abstraction. In: Proceed- 503
ings of the international conference on pattern recognition, 504
Cambridge, UK, pp 19–22 505
29. Torsello A, Hancock ER (2003) Computing approximate 506
tree edit distance using relaxation labeling. *Pattern Recognit* 507
Lett 24(8):1089–1097 508
30. van Eede M, Macrini D, Telea A, Sminchisescu C, Dick- 509
inson S (2006) Canonical skeletons for shape matching. 510
In: Proceedings of the international conference on pattern 511
recognition, Hong Kong, pp 64–69 512

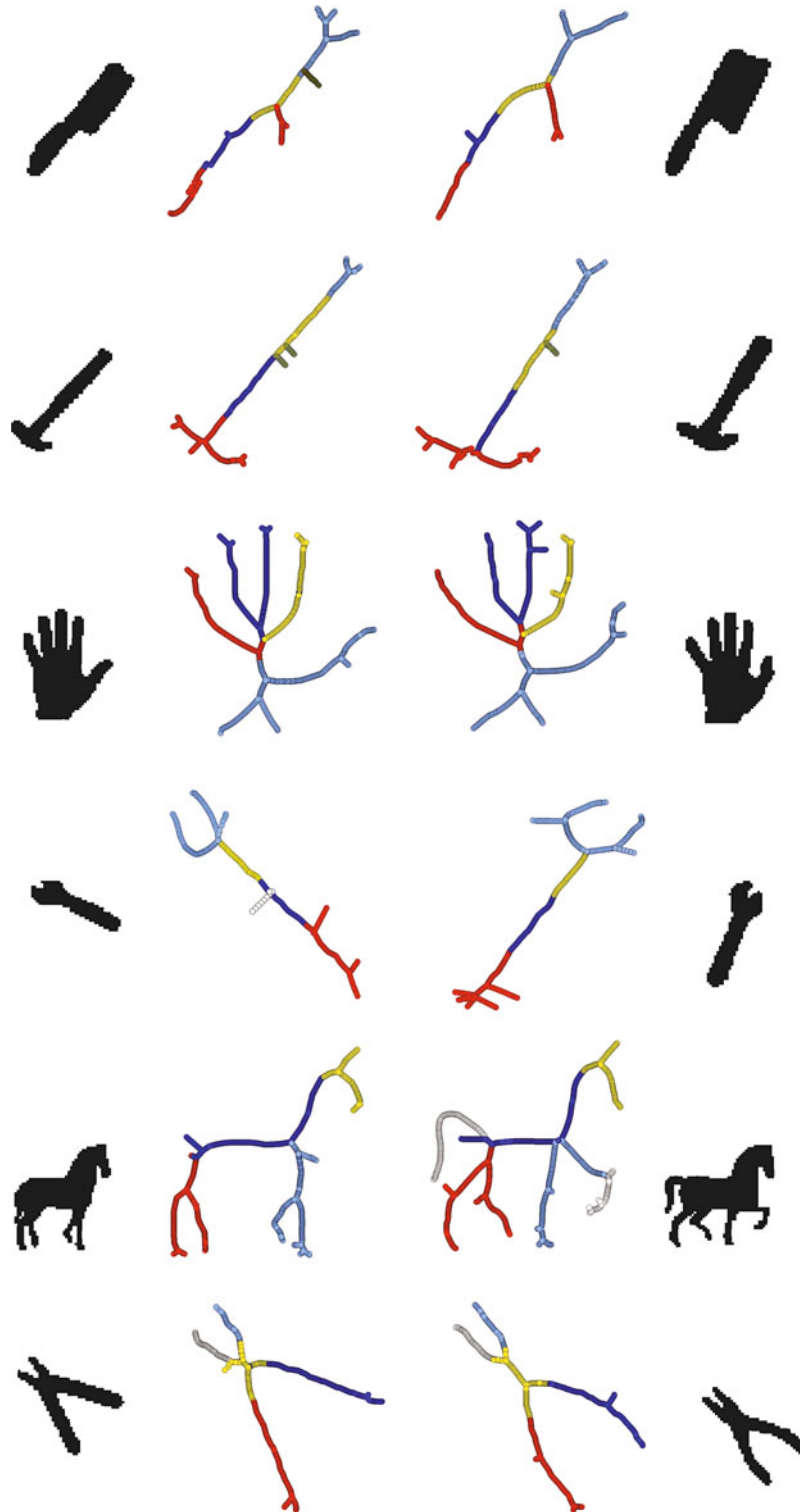


Shock Graph, Fig. 1 The shock graphs derived for two different views of a brush using the algorithm of Siddiqi et al. [24] are represented in the top row. The bottom row depicts the correspondences between nodes in the shock graphs computed by the matching algorithm

Corrected

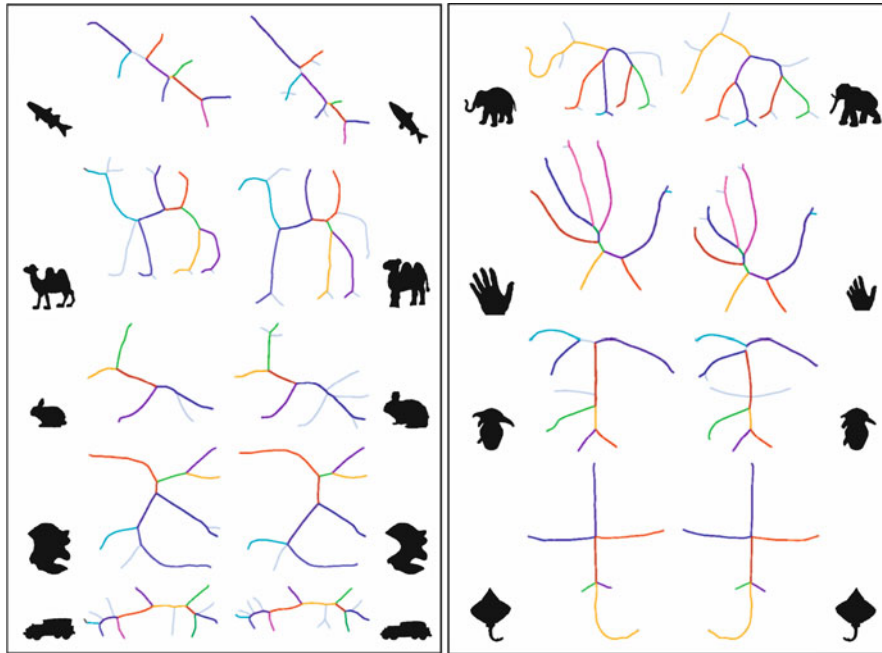
Instance	Distance to Class Prototype								
									
	0.02	2.17	4.48	3.55	2.96	0.21	4.58	14.33	10.01
	2.39	0.10	5.97	15.90	3.98	0.14	26.12	17.28	28.94
	10.89	4.72	2.08	12.24	3.12	2.15	19.73	10.11	12.64
	7.15	6.42	1.19	1.35	5.10	3.38	10.58	11.11	11.11
	4.08	7.72	2.98	1.49	4.26	4.14	26.60	13.54	14.21
	14.77	6.72	5.69	0.36	2.30	5.90	10.58	16.25	19.10
	7.86	8.90	5.94	0.74	1.59	1.10	10.81	10.39	16.08
	2.66	4.23	3.23	6.47	0.62	1.48	11.73	15.38	15.15
	3.18	5.31	1.25	4.64	0.60	1.30	14.18	17.22	9.08
	4.55	0.76	1.32	2.86	1.49	0.11	21.38	15.35	13.04
	6.77	19.46	22.11	13.27	8.21	29.50	0.15	5.12	5.03
	8.73	23.14	31.45	24.41	10.16	31.08	0.18	8.45	7.05
	12.46	19.0	27.40	14.58	24.26	17.10	8.85	7.49	16.93
	13.86	23.07	12.81	11.24	17.48	23.23	6.02	6.92	3.06
	15.73	21.28	14.10	12.46	19.56	19.21	9.53	7.12	5.06

Shock Graph, Fig. 2 Similarity between database and class prototypes computed using the algorithm of Siddiqi et al. [24]. In each row, a *box* is drawn around the most similar shape



Shock Graph, Fig. 3 The results of matching skeleton graphs for some pairs of shapes in the Rutgers Tools Database using the algorithm of Demirci et al. [9]. Corresponding segments are

shown using the same color. Observe that correspondences are intuitive in all cases



Shock Graph, Fig. 4 The matching results for a few shock graphs produced by the edit-distance algorithm of Sebastian et al. [18]. Matching shock branches are shown using the same

color, while the *gray* colored edges in the shock graphs indicate that they are spliced or contracted

Corrected